Study on Characteristic Variability of Weak Signal in High Density Seismic Acquisition*

Wujin Chen[1] and Anchu Wu[1]

Search and Discovery Article #41351 (2014)
Posted May 12, 2014

*Adapted from extended abstract prepared in conjunction with poster presentation at GEO-2014, 11th Middle East Geosciences Conference and Exhibition, 10-12 March 2014, GEO-2014©2014

[1]Sinopec Geophysical Corporation Shengli Branch, DongYing, China

Abstract

The seismic signal received by sensors is very weak because of absorption and attenuation by subsurface and deep layer during signal propagating. The high frequency component was much more serious absorbed and attenuated than low frequency component. The key issues for high-density seismic acquisition are to receive and identify low reflection coefficient or high frequency weak signal. In this paper the relationship between weak signal and subsurface, dominant frequency, offset and deep target layer was analyzed based on a typical elastic-viscoelastic earth model. Due to cut off frequency exists; it is very difficult to show the advantages of broadband frequency in high-density seismic acquisition in the area with strong subsurface attenuation and low S/N ratio. Good condition excitation can improve weak signal energy and give more contribution to broaden frequency band. The effective reflection coefficient can be better presented in small and middle receiver- source offset and can be well extracted to guide high-density data acquisition and processing.

Introduction

Point receivers, high spatial sampling and full wavefield broadband sampling are often used to acquire weak signal, the methods of broadening frequency band of seismic data and wavelet compressing is aimed to improve the resolution of stack and inversion interpretation. The amplitude of weak signal drown in noise is too weak to be visual resolved. Therefore, it is still an important subject to find the features of weak signals in high-density seismic acquisition.

Theory of Weak Signal Analysis

A simulation based on Zoppritz equation was processed to research the impact on the weak signal with the factors of near surface condition, target depth, source frequency and source-receiver offset.

Weak signal and ground absorption and attenuation

The near surface velocity model and Q factor model were created with up-hole, LVL and logging data in LJ area; the target layer model was created with velocity and density extracted from the seismic and well logging data. The depth of near surface ranges from ground surface to 100m below ground, and the depth of objectives range from 1,500m to 2,700m, the layer velocity was computed from well logging data (Figure 1). The Q factor was calculated with empiric formula below from Li Qing-Zhong (1993).

$$Q=14*(V_{IP}/1000)^{2.2}=3.156*V_p^{2.2}*10^{-6} \quad (1)$$

where V_p = P wave velocity.

A real Q factor model (Figure 3) was created with equation and velocity model (Figure 2) to study how much high frequency signals can be attenuated. A couple of simulation analysis were processed to study the weak signal character with the factors of near surface model and non near surface model considered, shooting at the depth 12.5m, receiving at surface, surface shooting and downhole receiving and changing the source excitation frequency.

Weak signal and target depth

Suppose the plane wave normally incident on a horizontal interface, the reflection coefficient and transmission coefficient can be derived according to Snell law.

$$R_{PP}=\frac{\rho_2 v_{P2}-\rho_1 v_{P1}}{\rho_2 v_{P2}+\rho_1 v_{P1}},\ R_{PS}=0 \quad (2)$$

$$T_{PP}=\frac{2\rho_1 v_{P1}}{\rho_2 v_{P2}+\rho_1 v_{P1}},\ T_{PS}=0 \quad (3)$$

Where R_{pp} is the reflection coefficient, T_{pp} is the transmission coefficient, ρ_1 is the first layer density, ρ_2 is the second layer density, v_{P1} is the first layer velocity, v_{P2} is the second layer medium velocity. Suppose the P wave normally incident from medium I to medium II with reflection coefficient of R_{PP} and transmission coefficient of T_{PP}, while P wave normally incident from medium II to medium I with reflection coefficient of R'_{PP} and transmission coefficient of T'_{PP} and,

$$T_{PP} \text{ x } T'_{PP} = 1-R^2_{PP} \quad (4)$$

In formula 4, the wave amplitude varies from the different directions through the same interface of the medium, which is called interface transmission loss.

In the surface seismic acquisition, the signals received by geophone sensors are effective reflection coefficient of the interfaces. Define the reflection coefficient R_n of n^{th} interface, downgoing transmission coefficient T_i of overlying interfaces and upgoing transmission coefficient T_i ', so T_i' is equal to:

$$R_e(\theta) = A_0 R_n(\theta) \prod_{i=1}^{n-1} T_i(\theta) T_i'(\theta_i') \tag{5}$$

Where $R_e(\theta)$ is the reflection coefficient with incident angle (θ), A_0 is the initial amplitude, T_i is the transmission coefficient with angle variations of i^{th} layer, T_i' is the transmission coefficient with angle variations which normally incident from medium II to medium I at i^{th} layer. When P wave vertical incidence, $\theta = 0$, R_e can be derived:

$$R_e = A_0 R_n \prod_{i=1}^{n-1} (1 - R_i^2) \tag{6}$$

Therefore, it is more accurate to use effective reflection coefficient to analyze weak signal.

Near Surface Absorption and Weak Signal

Viscoelastic medium wave equation forward modeling on earth model with P wave source surface centered, dominant frequency is 40Hz, sampling interval is 2.5m in lateral and sampling rate 0.25ms (Figure 4). In Figure 4, when near surface considered, the shape of reflections become fat and the frequency decreased. Therefore, it is shown that the high-frequency component is strongly absorbed by loose near surface, which degrades recognition ability to reflections.

Wave analysis

A further analysis on shot gather (Figure 5) with near offset 500m, the reflections shape become fat with phase distortion (Figure 5a). When the source was put at a depth of below 12.5m, the reflection wave shape becomes sharper (Figure 5b). When near surface model is ignored, the energy and resolutions becomes much higher (Figure 5c), note the direct arrival was already removed. Figure 6 shows the acoustic record comparison between with near surface model and without surface model. The time scale corresponds from 1.34s to 1.44s and 1.3s to 1.4s separately, the source dominant frequency is 50Hz. It shows that near surface absorption degrades the resolution to interfaces.

Frequency analysis

The amplitude spectrum in Figure 7 corresponds to Figure 5. Figure 7a shows the dominant frequency is 20Hz and high cut frequency is only 80Hz while considering the near surface. When the source is located at depth of 12.5m, the dominant frequency is increased. Without near

surface, the dominant frequency increases to 40Hz and high cut frequency extends to 100Hz (Figure 7c). We concluded that the near surface greatly attenuate the high-frequency component.

Energy analysis

A VSP forward modeling (Figure 8) was processed with geophone sensors vertical lay out. Figure 8a shows the viscoelastic record in vertical component Z direction with near surface considered and the depth range from surface to below 2,700m. The energy of first breaks decreased gradually as depth increased. Figure 8b shows the relationship between depth and maximum amplitude of first breaks in vertical component z direction. When the seismic wave penetrating from surface down to 100m depth below surface, the energy decreases greatly. However, as the target depth increased, the amplitude slowly decreased. Most of the energy is attenuated at near surface.

Weak Signal and Source Dominant Frequency

Model analysis with near surface model

Figure 9 shows viscoelastic record in vertical component with near surface at different dominant frequency, the reflections become slim as the dominant frequency increased, and the resolution increased as well. Figure10 shows the simulated record observed at offset 500m with near surface model, the source dominant frequency ranges from 10Hz to 100Hz, and the vertical component record is extracted at every 2Hz. The resolution increases with the dominant frequency increased. Figure 11 shows the amplitude spectrum with different dominant frequency at offset 500m with near surface considered. The dominant frequency increases and wave amplitude decreases with the excitation frequency increases, but it does not improve high frequency component and bandwidth. Figure 12 shows the power spectrum at near offset 500m with time window 0.83s to 0.95s and depth at 900m.

The dominant frequency increases in power spectrum with source dominant frequency increases. When the source dominant frequency starts from 10Hz, the reflections dominant frequency increases correspondingly, but when the source dominant frequency increases below 30Hz, the dominant frequency increases greatly, but the source dominant frequency reaches above 50Hz, the dominant frequency of reflections increases slowly. Therefore, it is very difficult to improve high frequency component because of the absorption and attenuation by near surface even though the excitation frequency increased.

Analysis without near surface model

Figure 13 shows the power spectrum at offset 500m without the near surface model. The dominant frequency increases with source frequency linear increasing from 10Hz, and the high frequency component are not absorbed. Figure 14 shows the acoustic record comparison between dominant frequency 100Hz and 50Hz without surface model, the time scale is 1.6s to 1.7s.While dominant frequency increased, the vertical resolution increased, at time 1.625s, two interfaces can be resolved with dominant frequency 100Hz while dominant frequency 50Hz cannot. Figure 15 shows the record of thin interbed response. The viscoelastic record at trace number 120 was extracted. Weak signal can be resolved

when the dominant frequency increases. So increasing source dominant frequency weak signal energy can be improved with broad frequency at the area where near surface absorption and attenuation is weak.

Weak Signal and Receiver- Source Offset

Effective reflection and offset

Effective reflection coefficient with incident angle (offset) was computed on weak reflection layer at depth 2,400m according Zoppritz equation (Figure 16). Figure 16 shows the effective reflection coefficient reduced gradually while incidence angle (offset) increasing, and it reduced greatly when the incidence angle close to critical angle. When considering near surface model, the critical angle is 4.3°, which the offset is 3,300m, so the primary wave cannot transmit to this layer. When there is no near surface effect, the critical angle is 21.7° and the offset is 3,538m. The critical angle and reflection coefficient become smaller with near surface model than that without near surface model.

According to Zoppritz equation in formula (5), the critical angle is analyzed with variations of layer depth (Figure 17). The results with near surface model are shown in Figure 17a. The critical angle of primary wave with near surface model decreases from 70.2° at surface to 4.2° at deep layer. The signal received from long offset with big incidence angle is very limited. In addition, the critical angle reduces very quickly from 70.2° at near surface to 10.4°. So signals from deep target are strongly shielded by thick near surface. Because of velocity variations below 2,000m (Figure 1 and Figure 2), the critical angle steps drop greatly. Therefore, the deep layers with high velocity have strong shielding effect on the primary waves with big incidence angles. Without near surface, the critical angle drops slowly (Figure 17b).

Because of AVO effect, even at the same interface, the amplitude of the reflected signal from different offset is different. Figure 18 shows the amplitude frequency of deep target with source dominant frequency 40Hz. While the offset is less than 1000m, the tuning effect is weak; the band pass is wide with better AVO effect. When the offset is more than 1,400m, the tuning effect is strong and band pass is narrow. So middle–small offset will give more benefit for weak signal to be extracted for processing.

Energy and frequency of weak signal and offset

What is the relationship between weak signal energy, frequency and offset? The energy of reflected signal is extracted shown in Figure 19 with source frequency from 30Hz to 80Hz and offset from 0 to 1,500m, and the reflected energy is shown in Figure 20 and Figure 21 related to offset and source frequency. The reflected energy declines with the offset increased in both models. The area with strong reflected energy is obvious small with the offset less than 500m with near surface model, and the frequency in 500m-1,000m reduces to 10-15Hz (Figure 20). However, without near surface model, the best observing area for weak signal at below 45Hz is at near offset less than 1,500m, and the stronger energy with frequency more than 50Hz can be observed at offset less than 500m.

Weak Signal and Deep Target

The original reflection coefficient and effective reflection coefficient (Figure 22) are calculated according Formula (2) and (6). The maximum absolute value of original reflection coefficient is 0.1395 with vertical incidence, and there are 173 interfaces with absolute value less than 5% of maximum value, which is only 36.0% of all values (Figure 22a). While the maximum absolute value of effective reflection coefficient is 0.1042, the absolute value, which is less than 5% of maximum value, is only 39.5% of all values (Figure 22b). So the transmitting loss is relative small for weak signal with vertical incidence, the shape character is similar between original reflection coefficient and effective reflection coefficient.

Figure 23 shows the effective reflection coefficient with dominant frequency 50Hz, the time scale is 1.3s to 2.0s. The yellow color represents the ratio of absolute value to maximum is more than 30%, the green color represents the ratio of absolute value to maximum is more than 20%, the blue color represents the ratio of absolute value to maximum is more than 10%, the red color represents the ratio of absolute value to maximum is more than 5%, the black color represents the ratio of absolute value to maximum is less than 5%. Within the deep target with 481 interfaces, 86 interfaces can be resolved through the waveform. When the seismic waves propagate with a certain incidence angle, the transmission coefficient decreases, and the effective reflection coefficient also decreases along with the target depth increases, which the propagating time becomes longer. Therefore, the small source to receiver offset is the best range to receiver weak signal from deep layers.

Figure 24a to c corresponds to weak signal at target layer depth 1,725m, 2,105m and 2,657m. The figure only shows the layers with the ratio of absolute effective coefficient to maximum is less than 2%, the blue curve shows the record before removing weak signals, the green curve shows the record after removing weak signals. The peak wave amplitude has a little drop when the weak signal removed. The weak signal layer at depth 1,725m (Figure 24a) is attenuated and makes the adjacent peak wave amplitude drop. Therefore, the energy of weak signal decreases with target layer depth increases. Figure 24 shows that during attribute extraction and interpretation, if the thin interbed layer with less changes of lithology, the time window to be selected with strong reflections layers should be avoided for frequency and spectrum analysis, otherwise it is very difficult to show the weak signal in the spectrum.

Conclusions

Near surface has strong absorption to seismic signal, there are different cut-off frequency at different areas and at different targets. The cut off frequency is low at area with strong absorption, so it is very difficult to broaden the frequency band even with digital geophone sensors. At area with weak absorption at near surface, the weak signal energy and bandwidth can be better improved through increasing the source frequency. Because of critical angle, absorption and attenuation, the energy of weak signal will be mainly concentrated at mid-small offset, which is the best area for signal analysis; it is not a good choice to pick weak signal at the far offset. In addition, during the phase of survey design for high density, the field parameters should be optimized with a consideration of characteristics of weak signal.

Reference Cited

Li, Qing-Zhong, 1993, To accurate exploration road: Petroleum Industry Press, Beijing, China, p. 31-38.

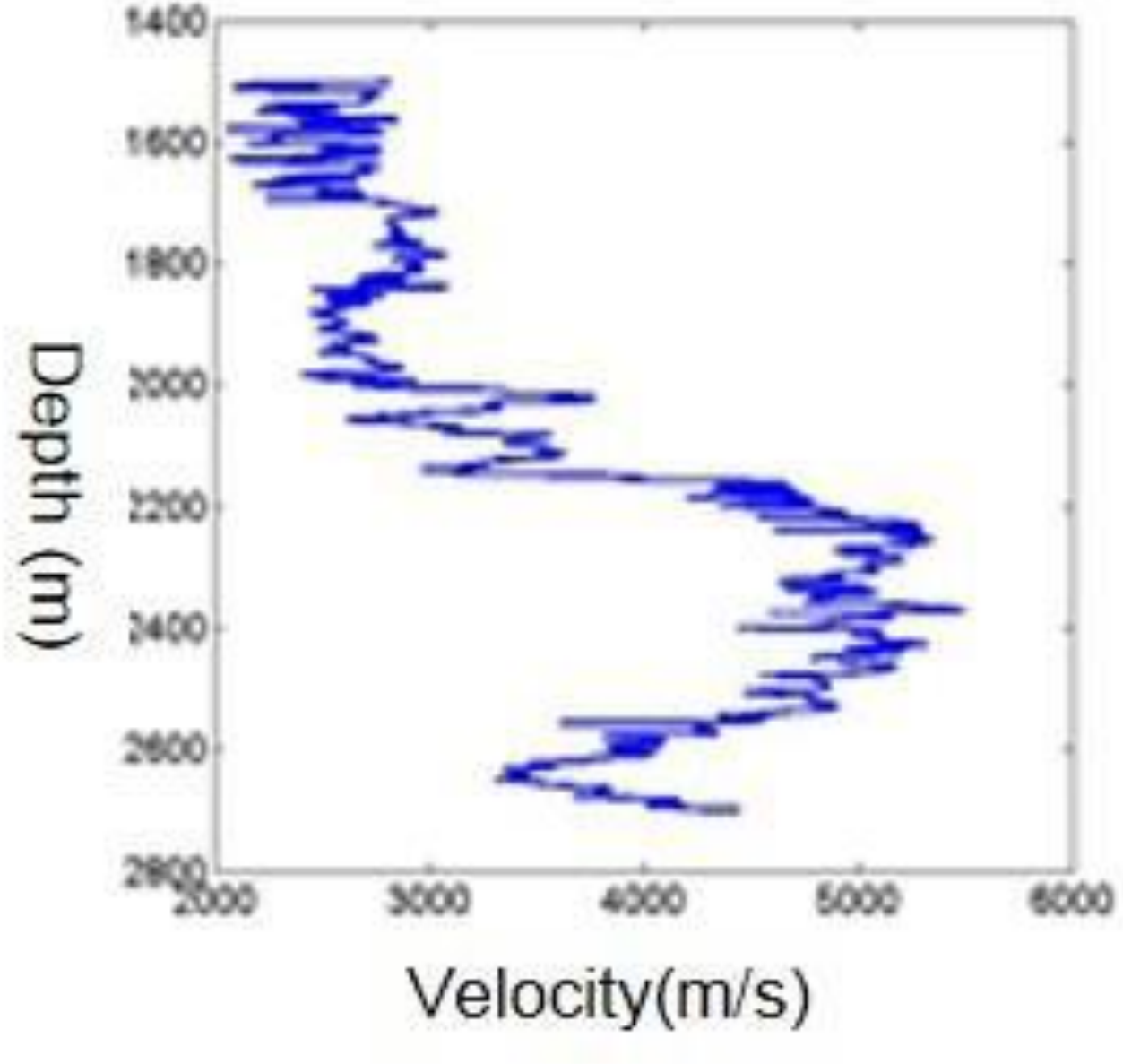

Figure 1. Velocity results for well logging data.

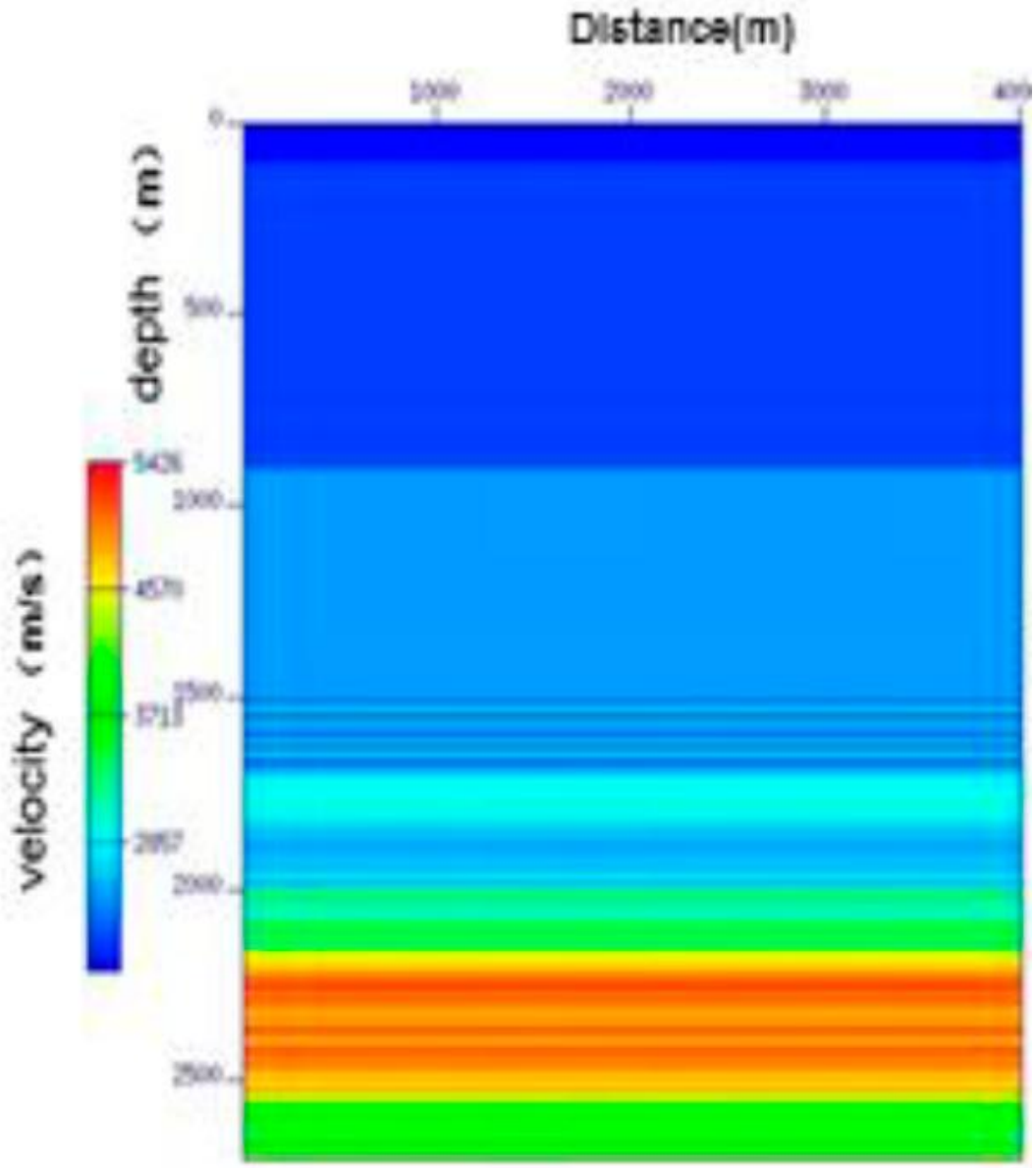

Figure 2. Velocity model.

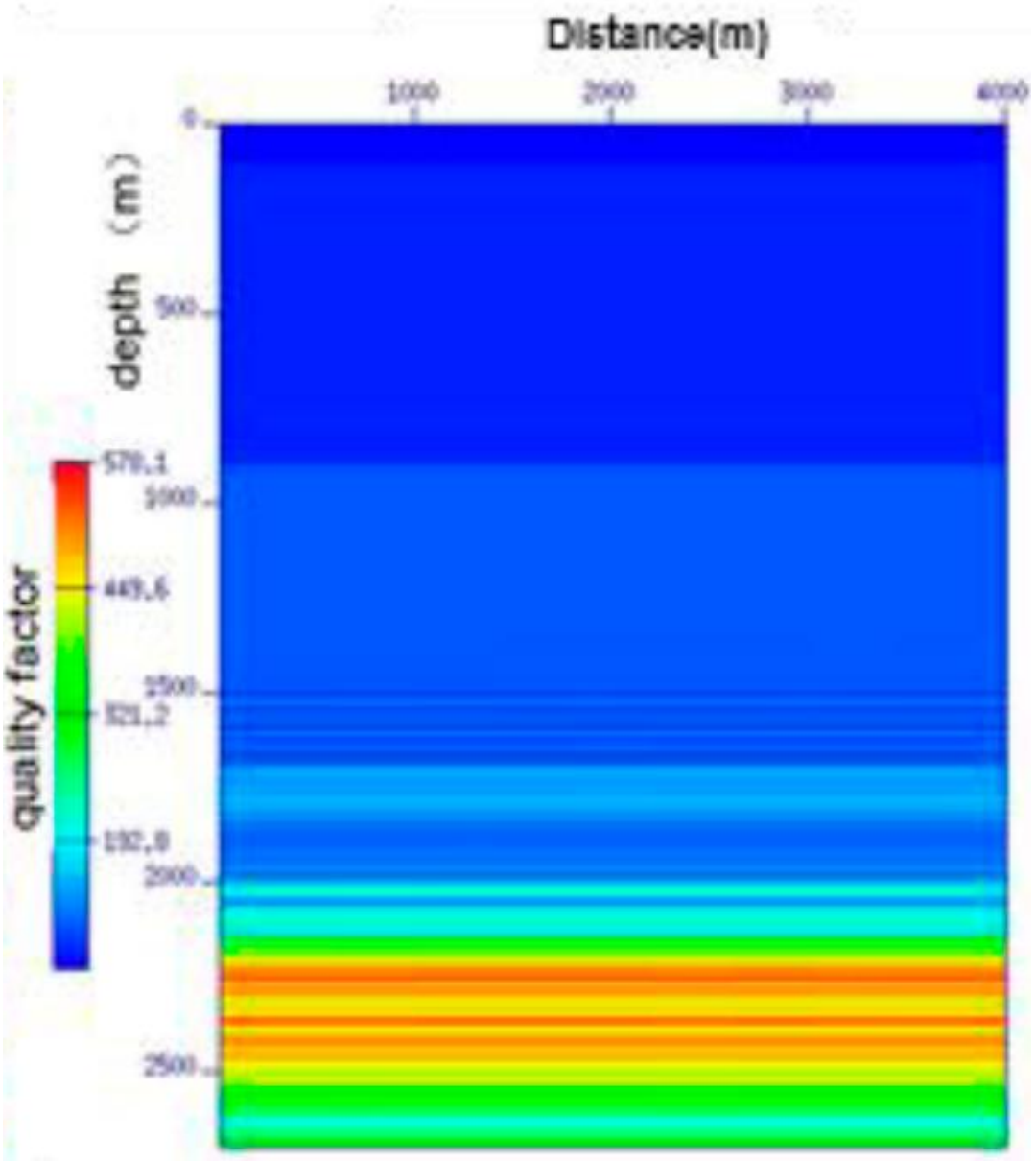

Figure 3. Q factor model.

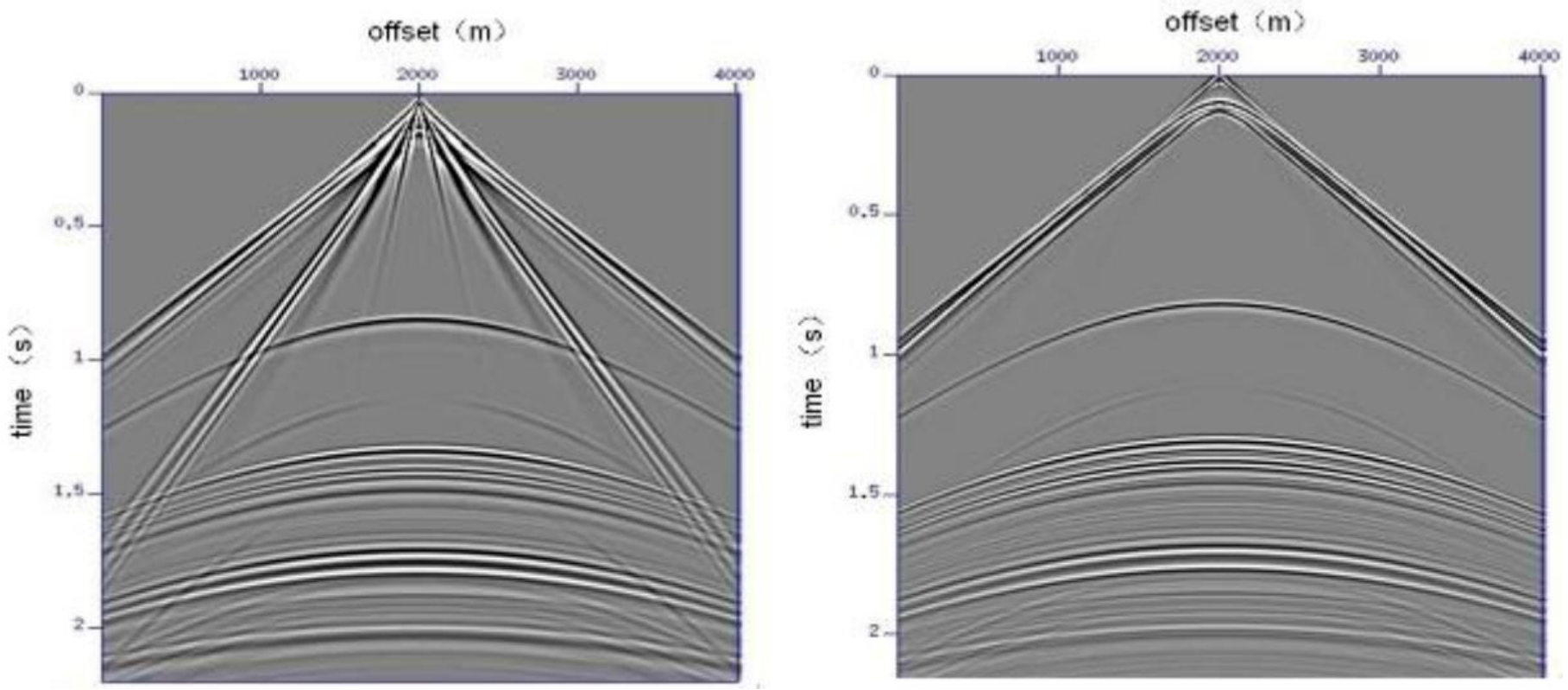

Figure 4. Wavefield synthetic shot gather comparison with near surface (a: left) and without near surface (b: right).

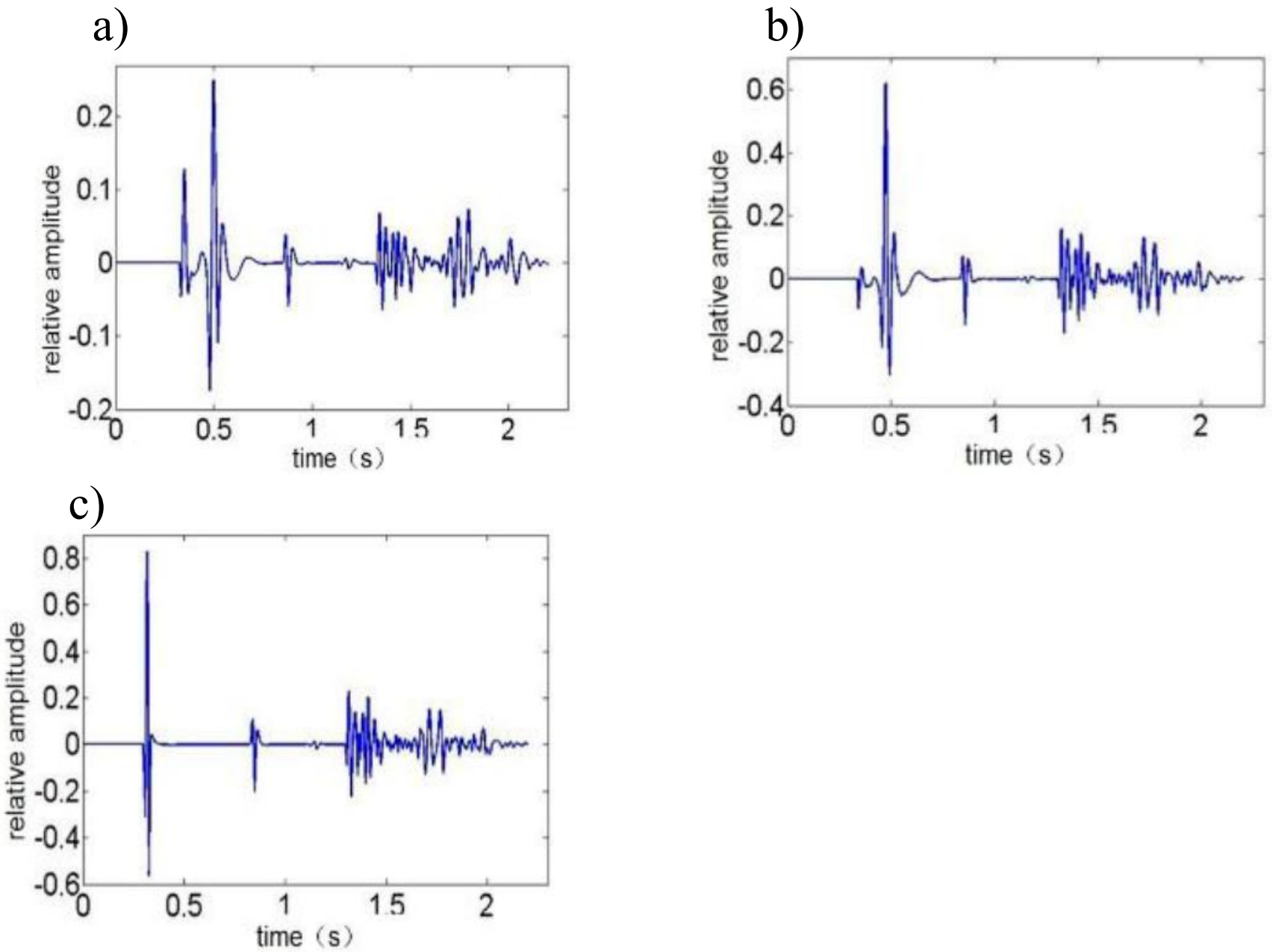

Figure 5. Shot gather at near offset 500m. Source at surface (a: top left), source at below 12.5m depth (b: top right), and without near surface model (c: bottom).

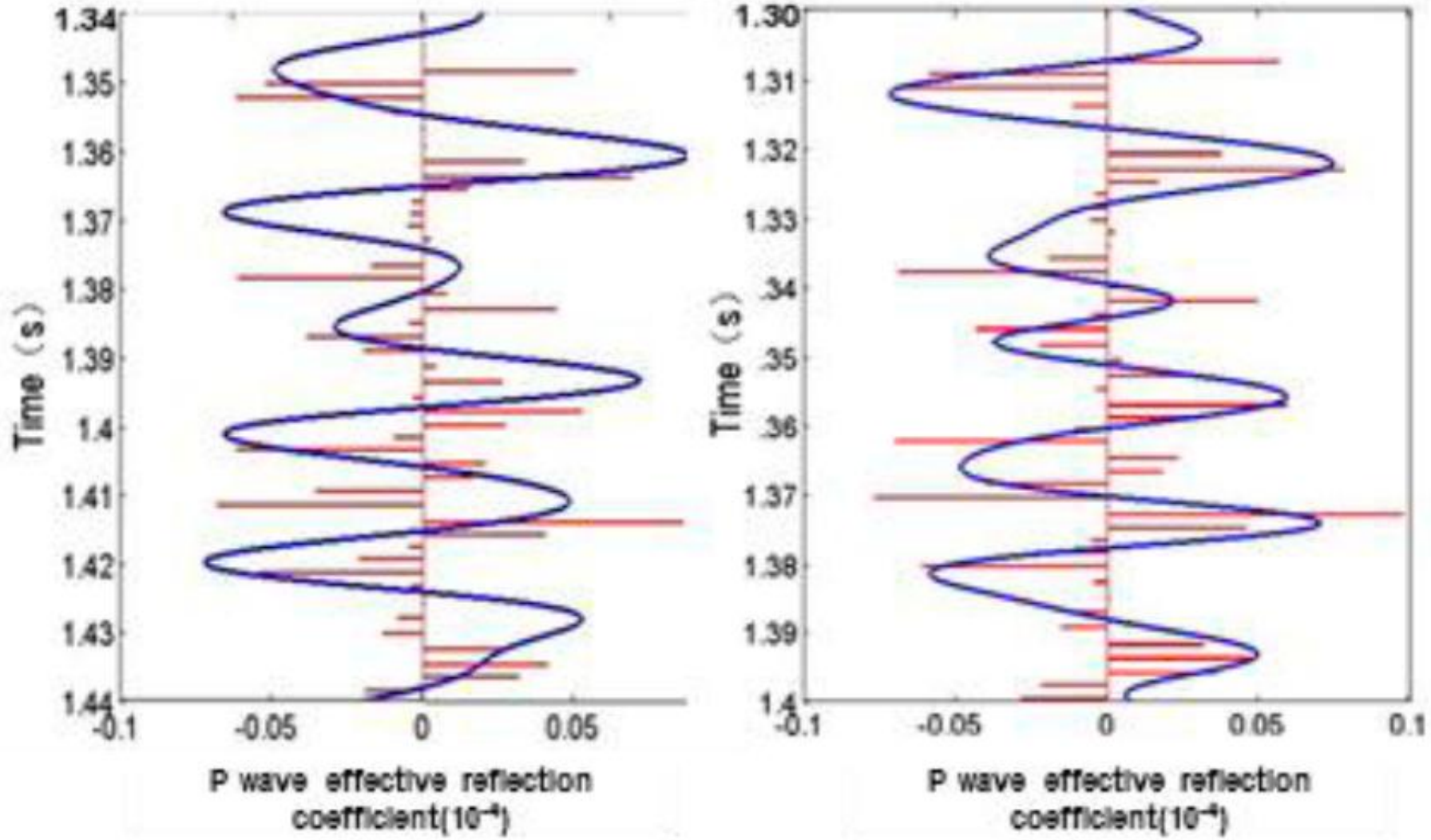

Figure 6. Acoustic record comparison with near surface model (a: left) and without near surface model (b: right)

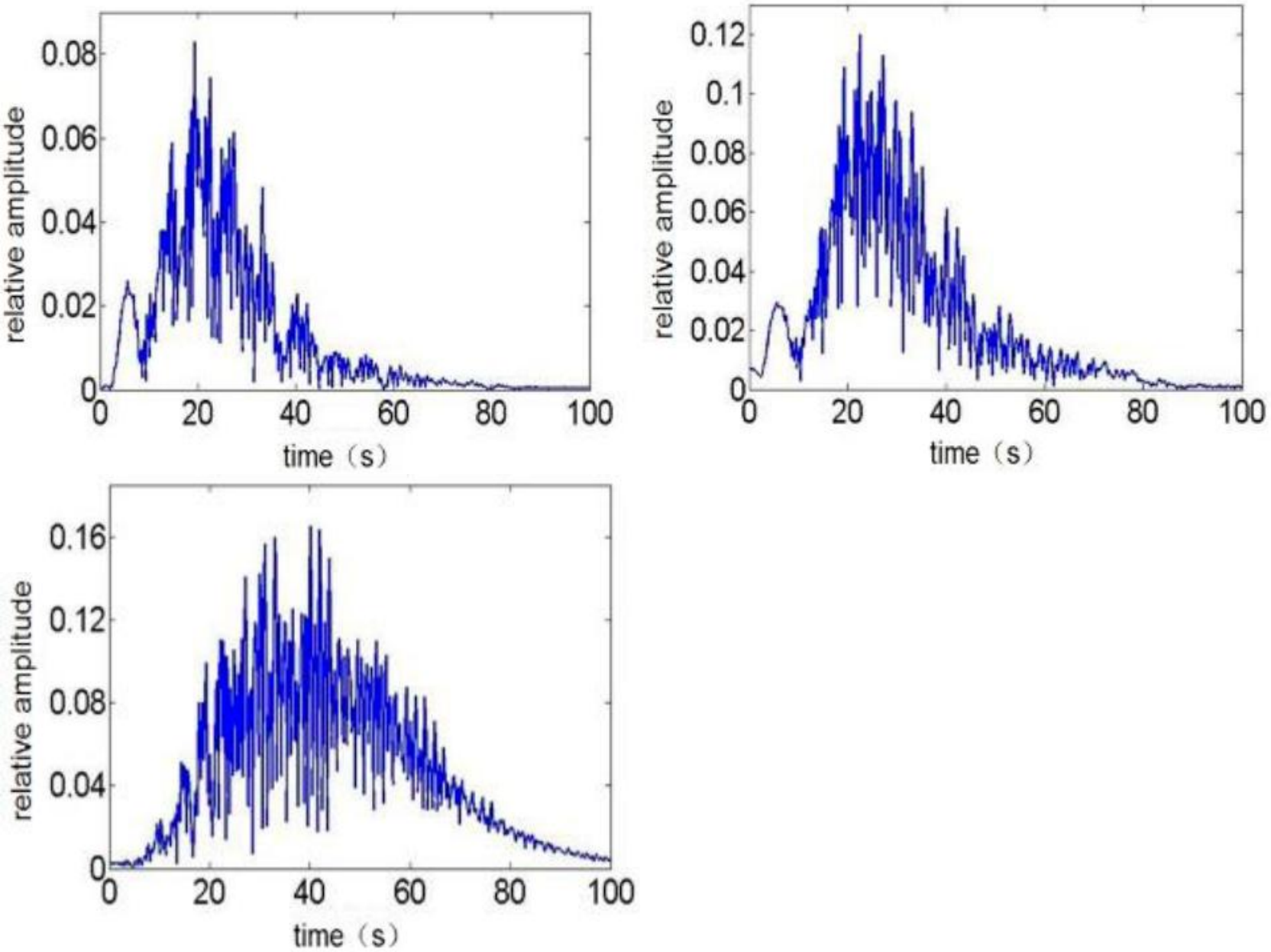

Figure 7. Amplitude spectrum at near offset 500m with near surface model (a: top left), source at 12.5m below surface (b: top right), and without near surface model (c: bottom).

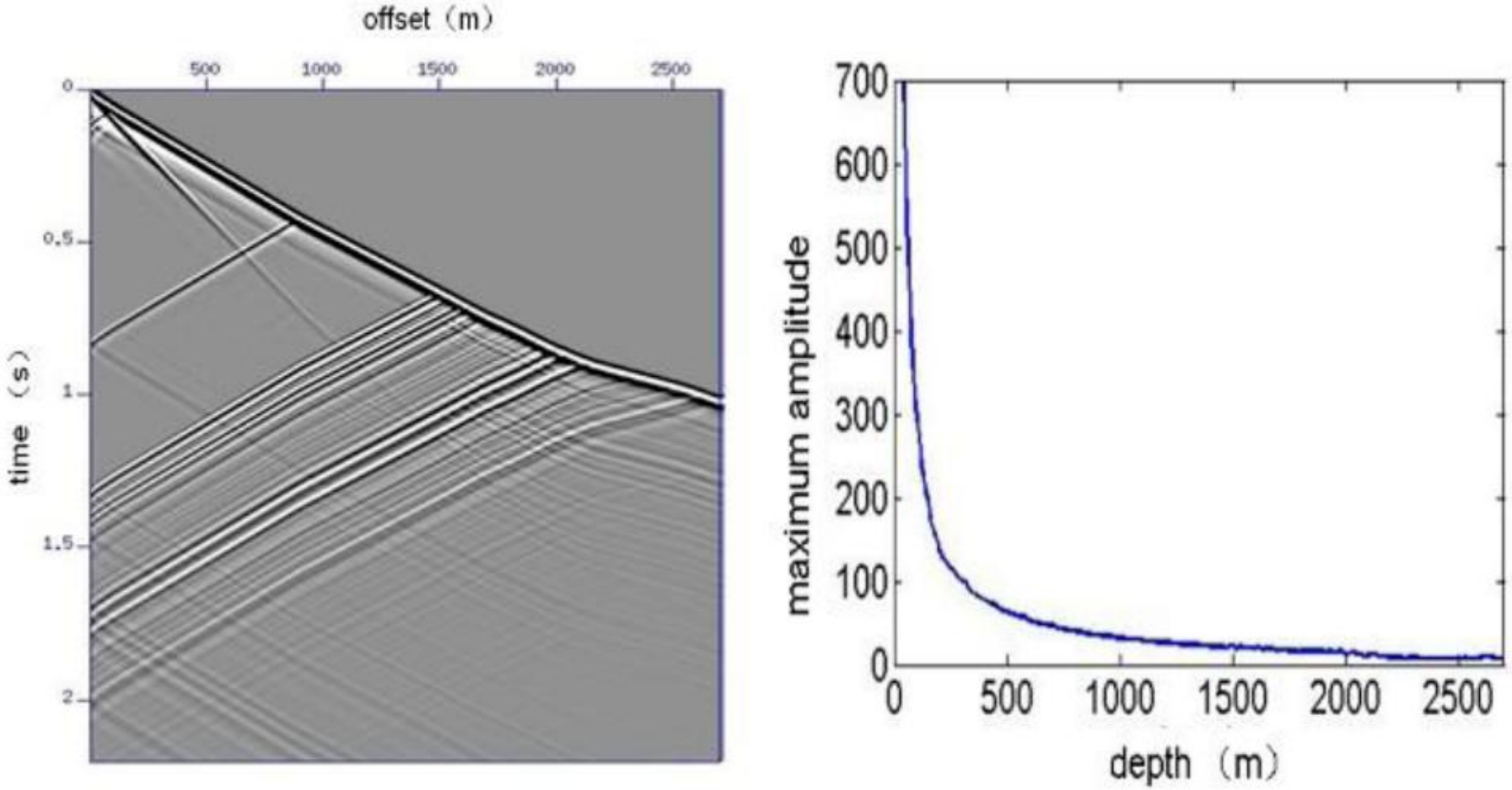

Figure 8. VSP wavefield simulation analysis: VSP record (a: left), amplitude of first break (b: right).

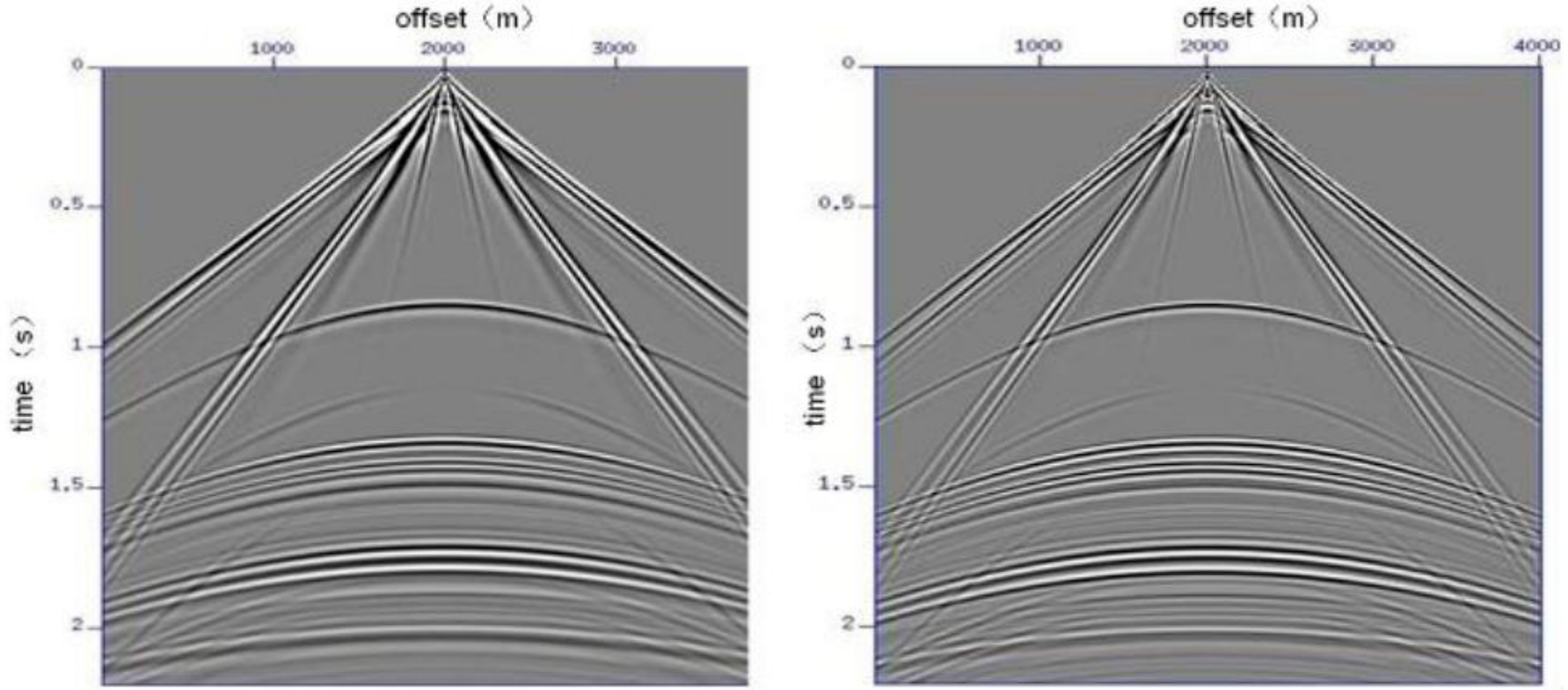

Figure 9. Synthetic shot gather at different dominant frequency: 40Hz (a: left) and 80Hz (b: right).

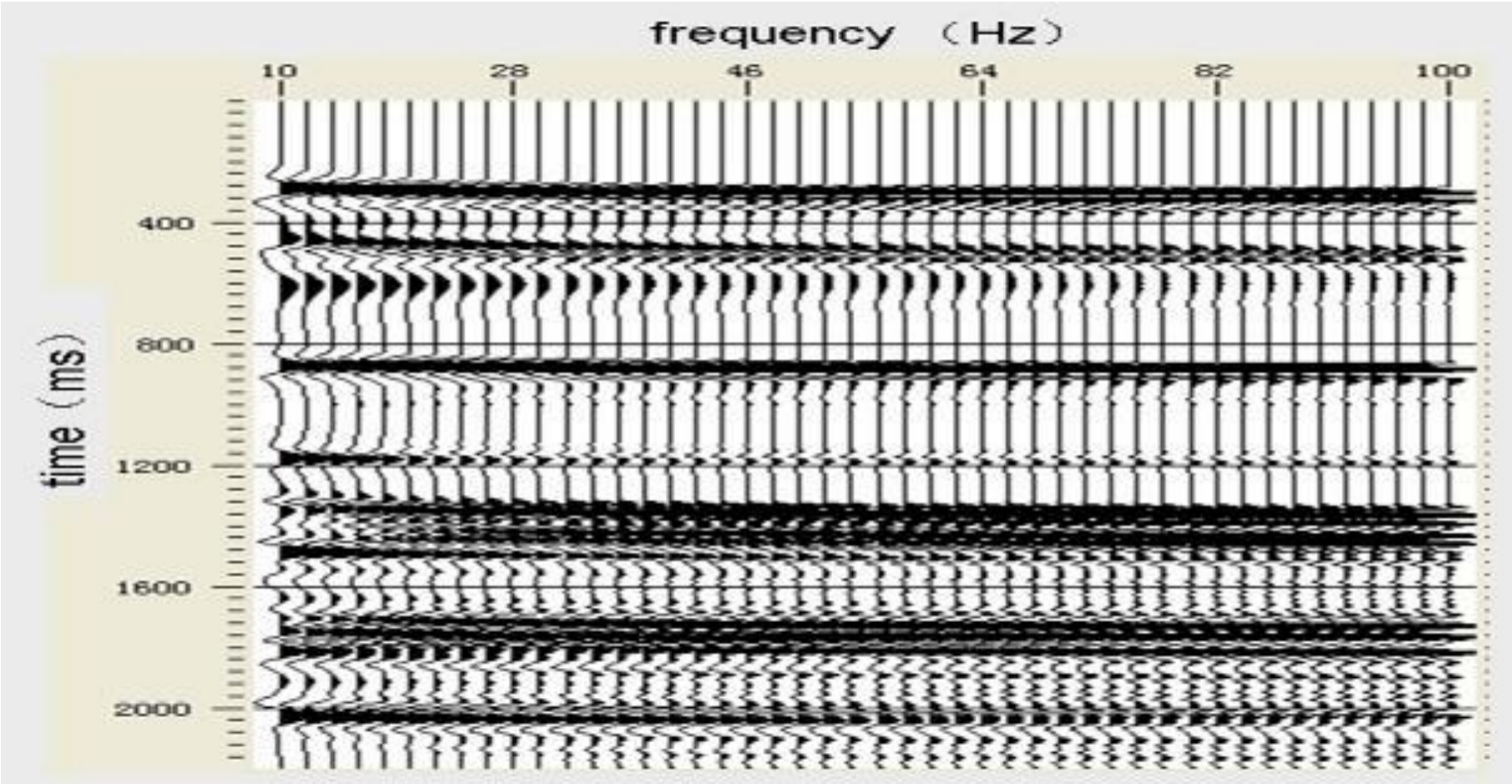

Figure 10. Synthetic viscoelastic record at offset 500m (vertical component).

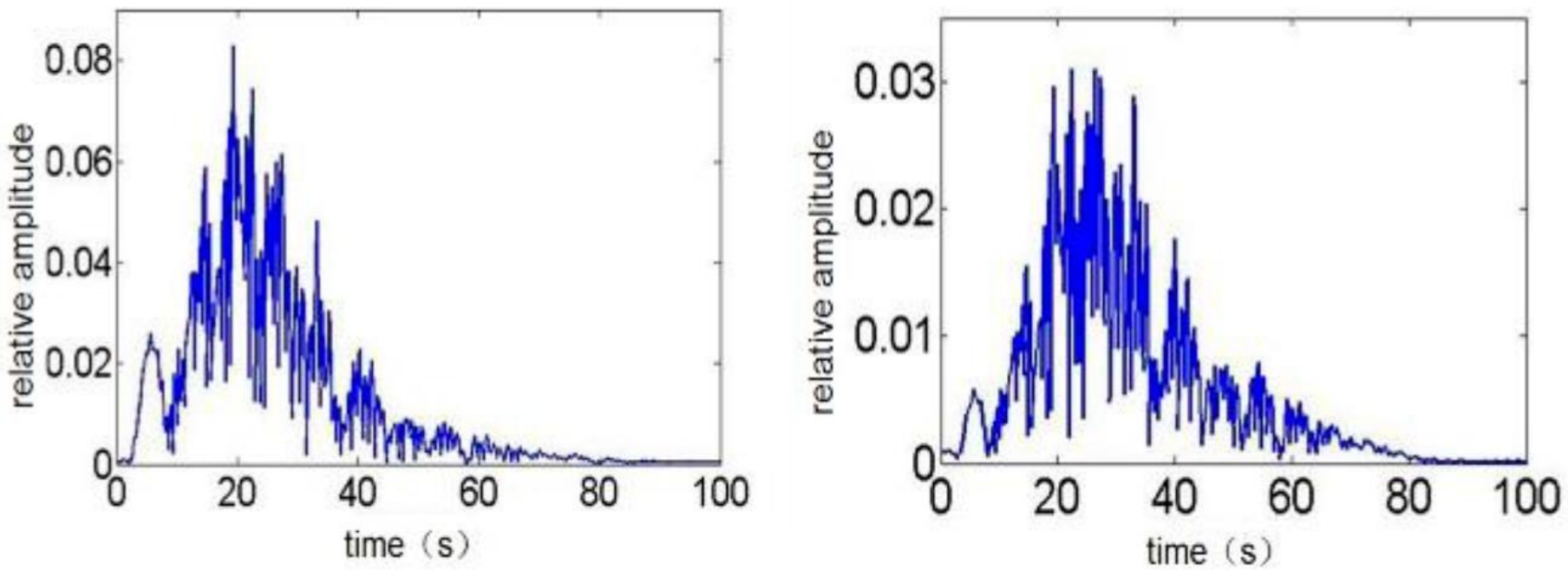

Figure 11. Amplitude spectrum at offset 500m: 40Hz (a: left) and 80Hz (b: right).

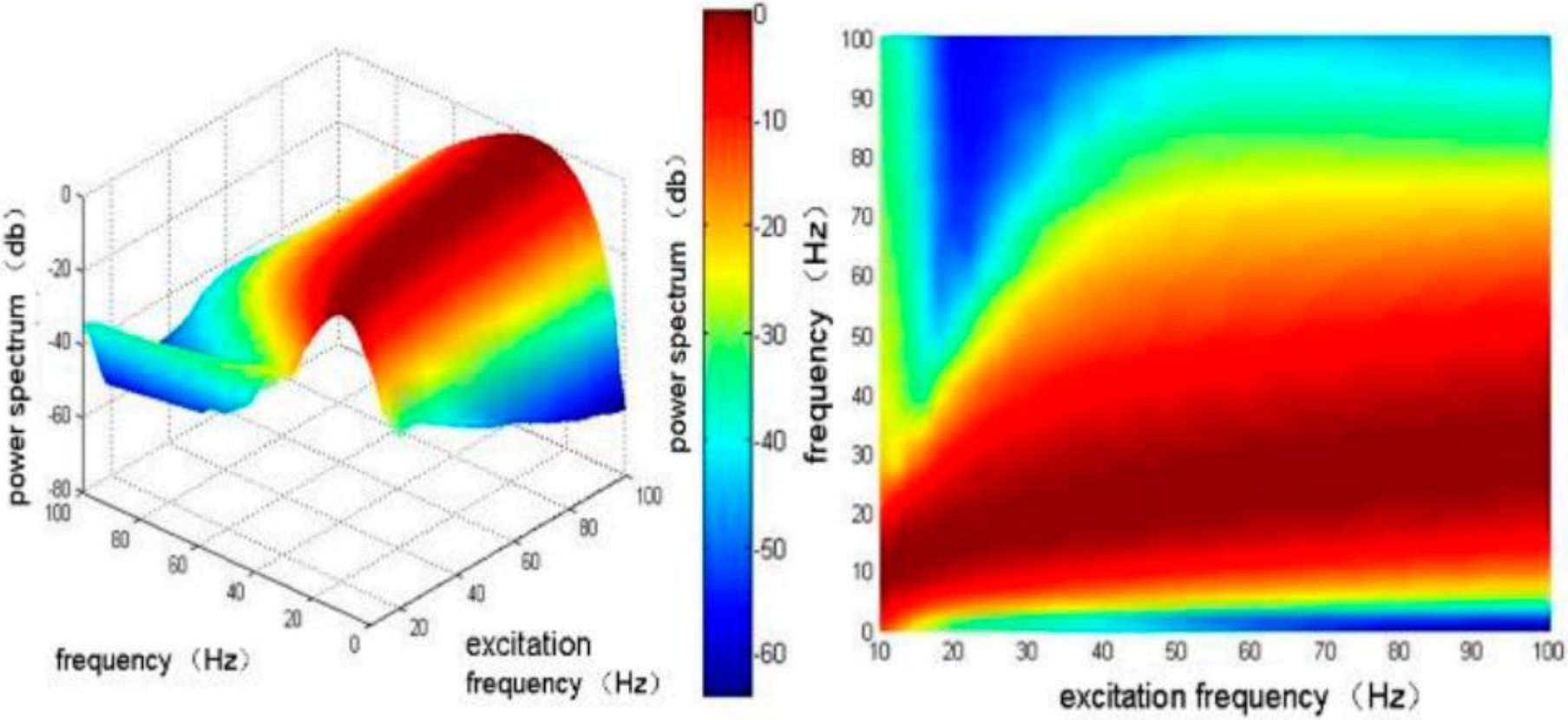

Figure 12. Power spectrum at near offset 500m: 3D view (a: left) and 2D view (b: right).

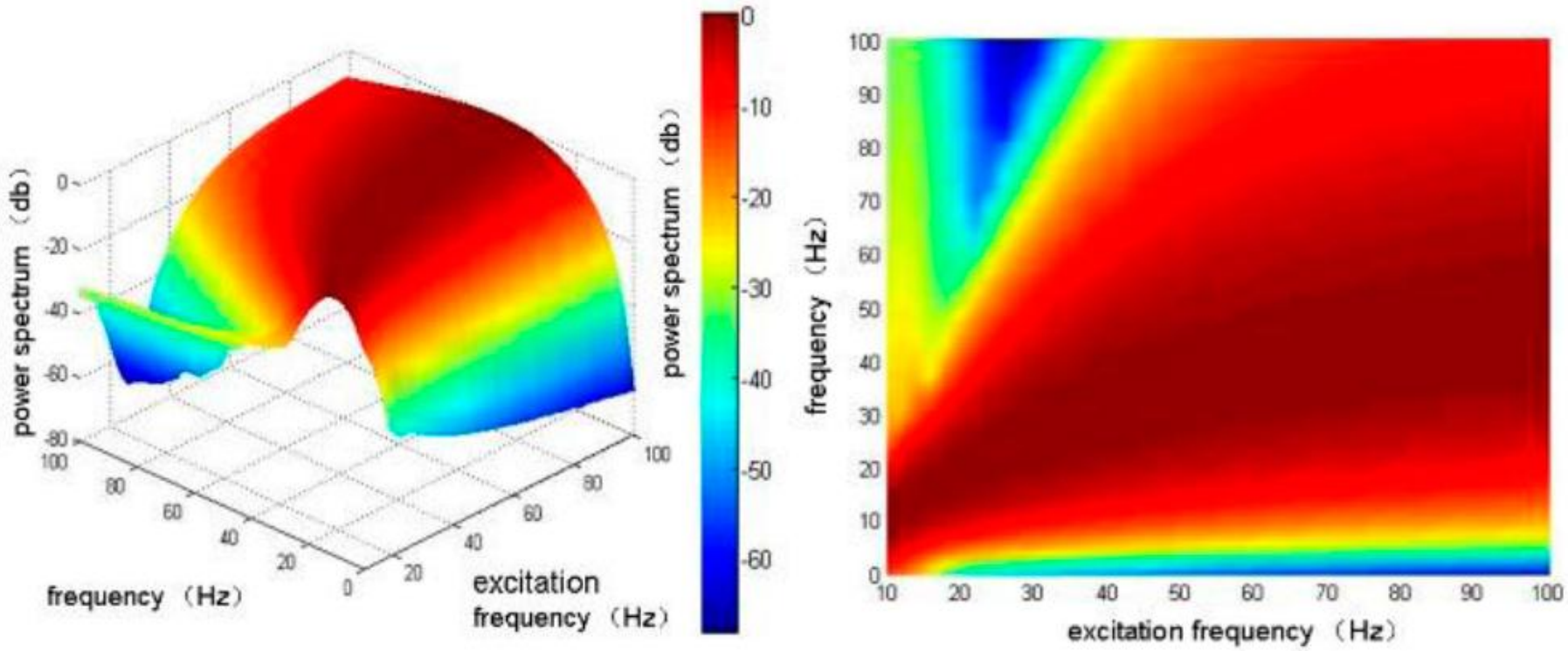

Figure 13. Power spectrum at offset 500m without near surface model: a power spectrum 3D view (a: left) and 2D View (b: right).

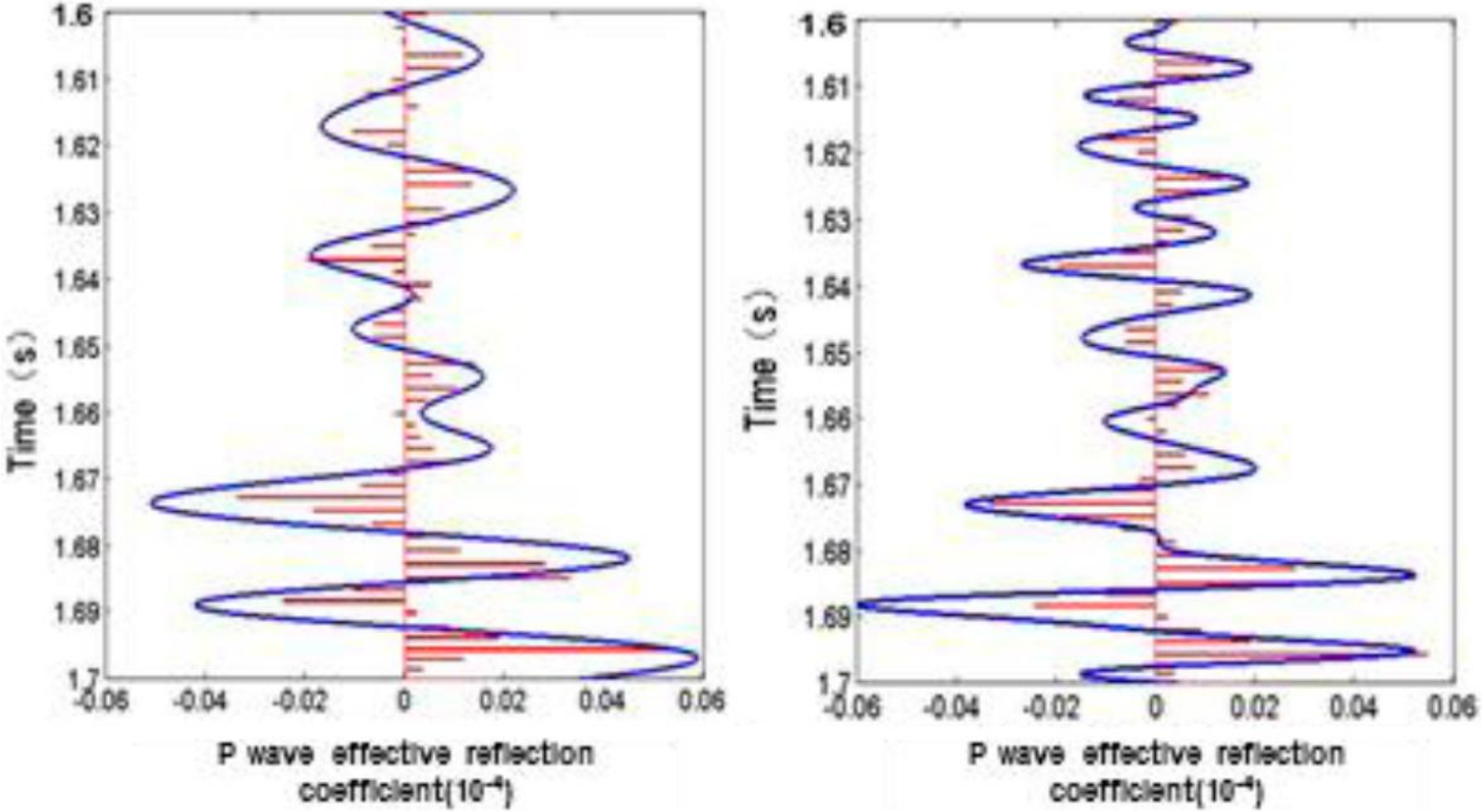

Figure 14. Acoustic record comparison: 50Hz (a: left) and 100Hz (b: right).

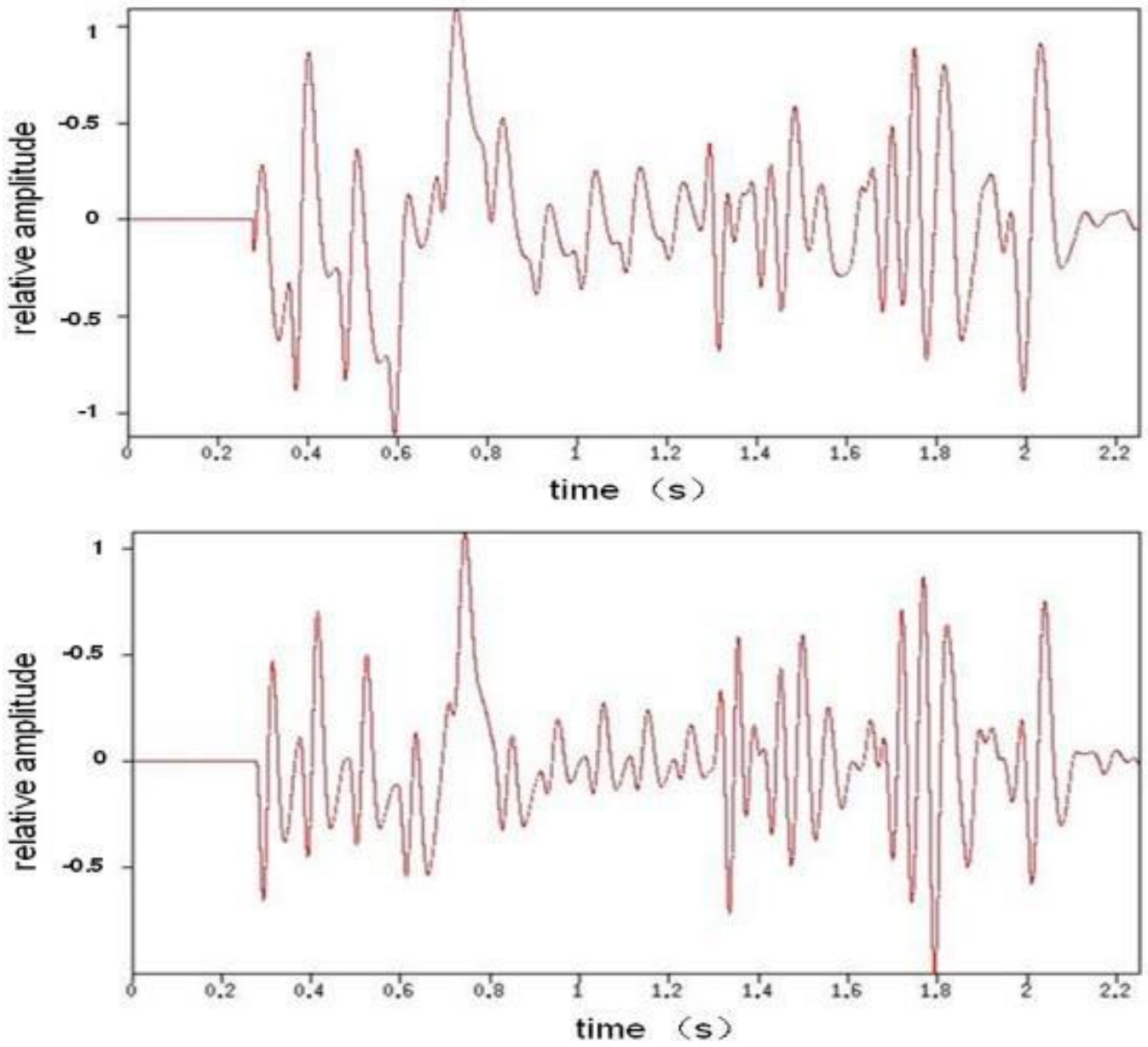

Figure 15. Vertical component record at trace number 120: wavelet dominant frequency 40Hz (a: top) and wavelet dominant frequency 80Hz (b: bottom).

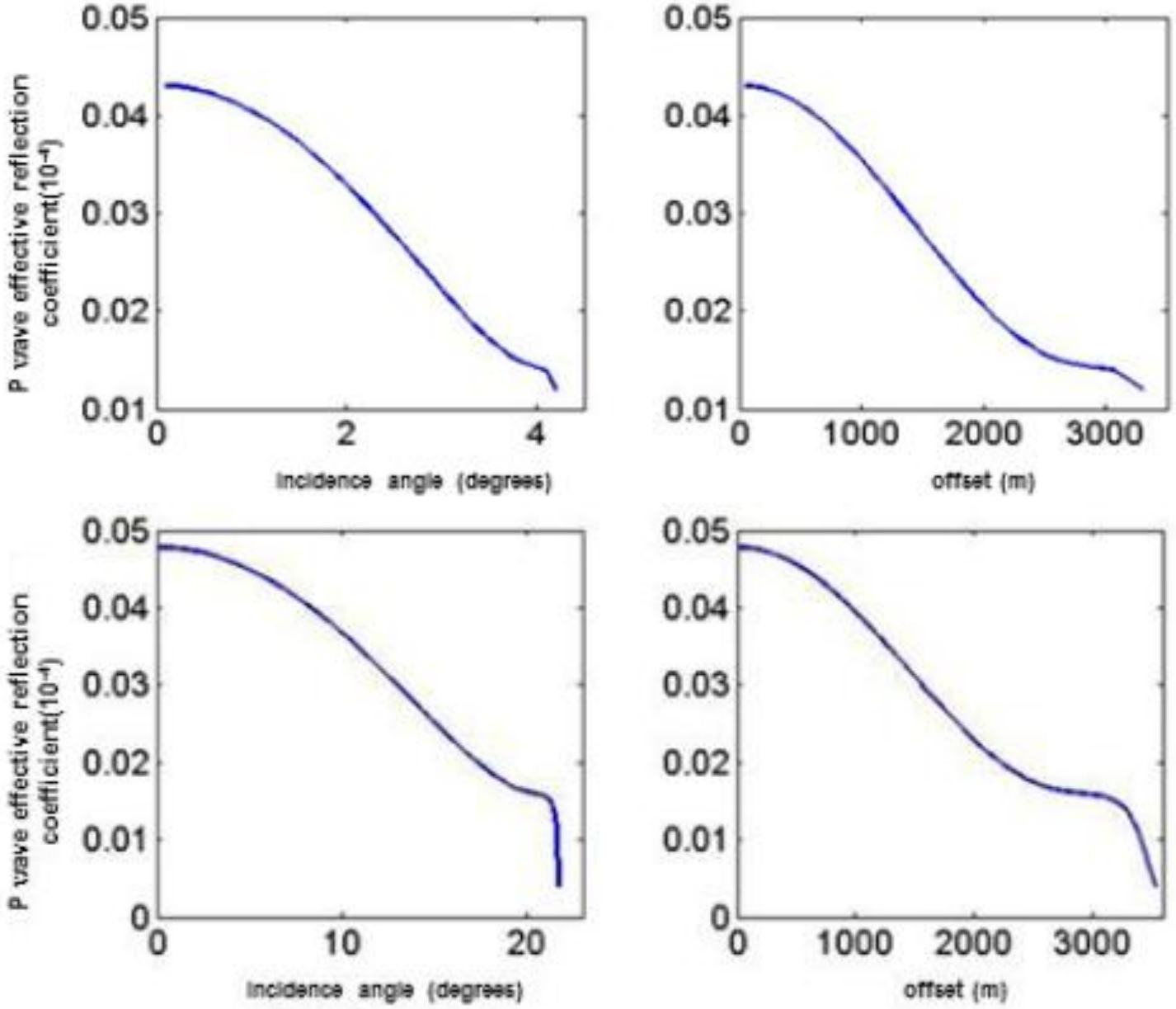

Figure 16. Effective reflection coefficient at 2400m: with near surface model (a: top) and without near surface model (b: bottom).

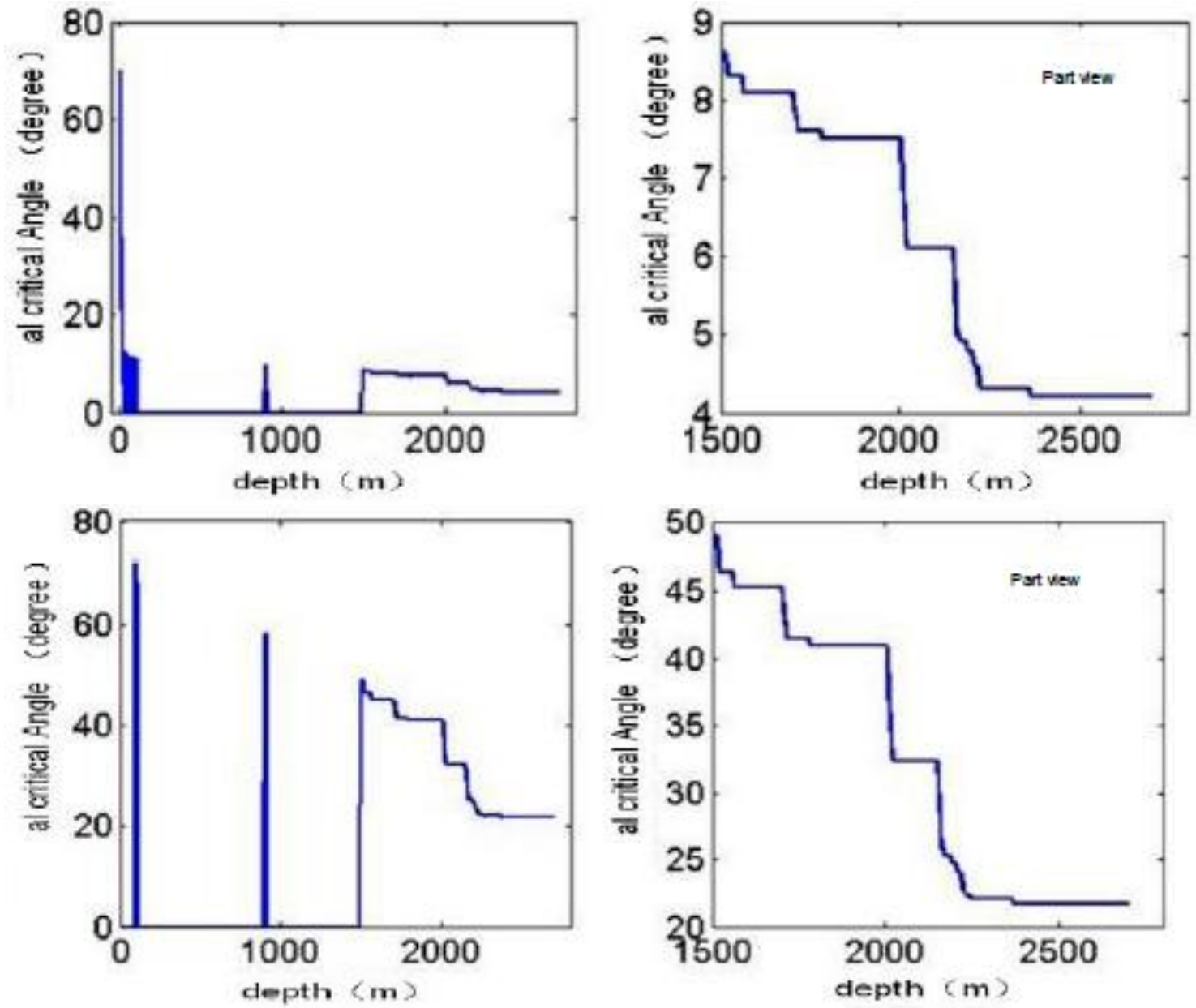

Figure 17. Critical angle and layer depth: with near surface model (a: top) and without near surface model Figure 18 Amplitude & Frequency at deep layer Cubic view Plane view (b: bottom).

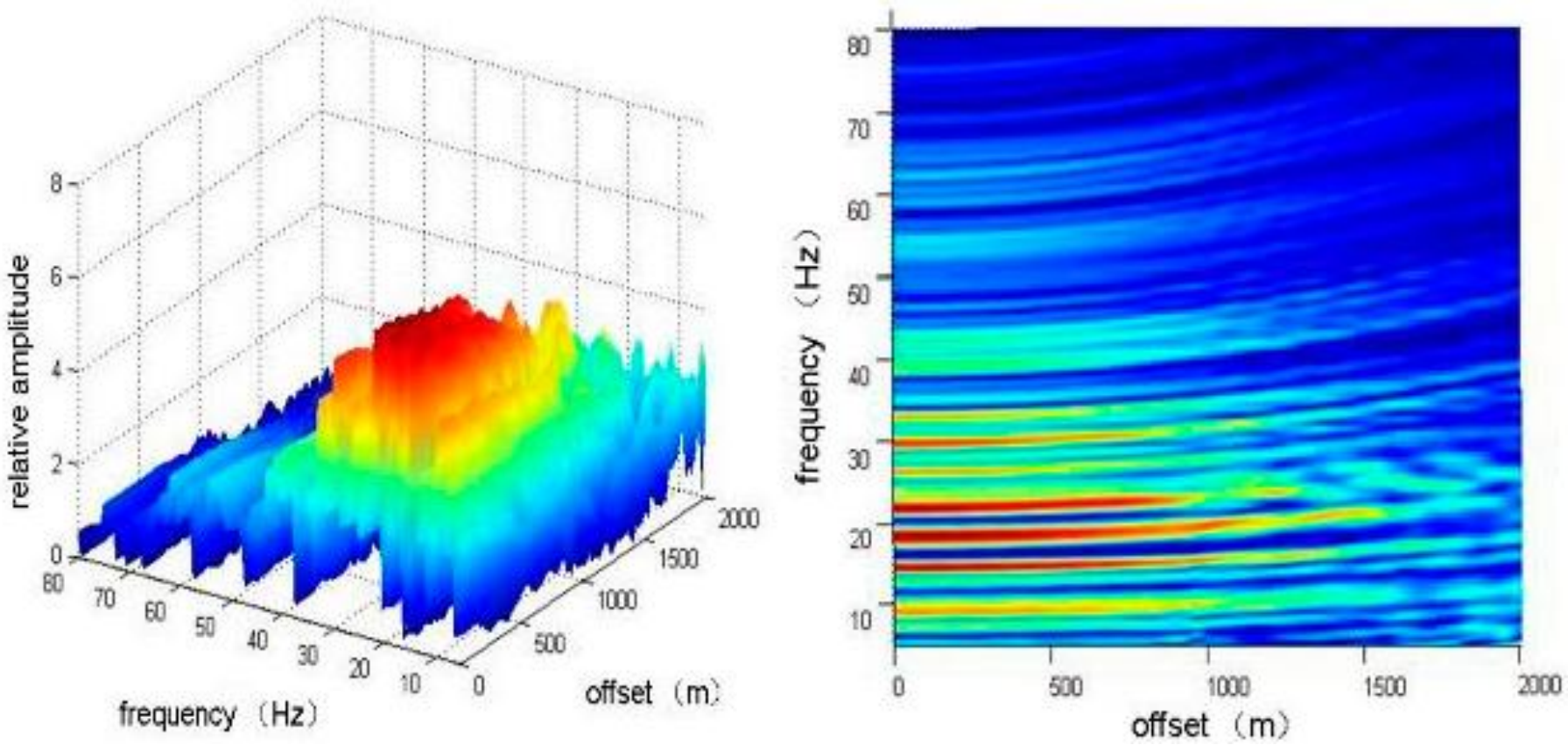

Figure 18. Amplitude & Frequency at deep layer: Cubic view (a: top) and Plane view (b: bottom).

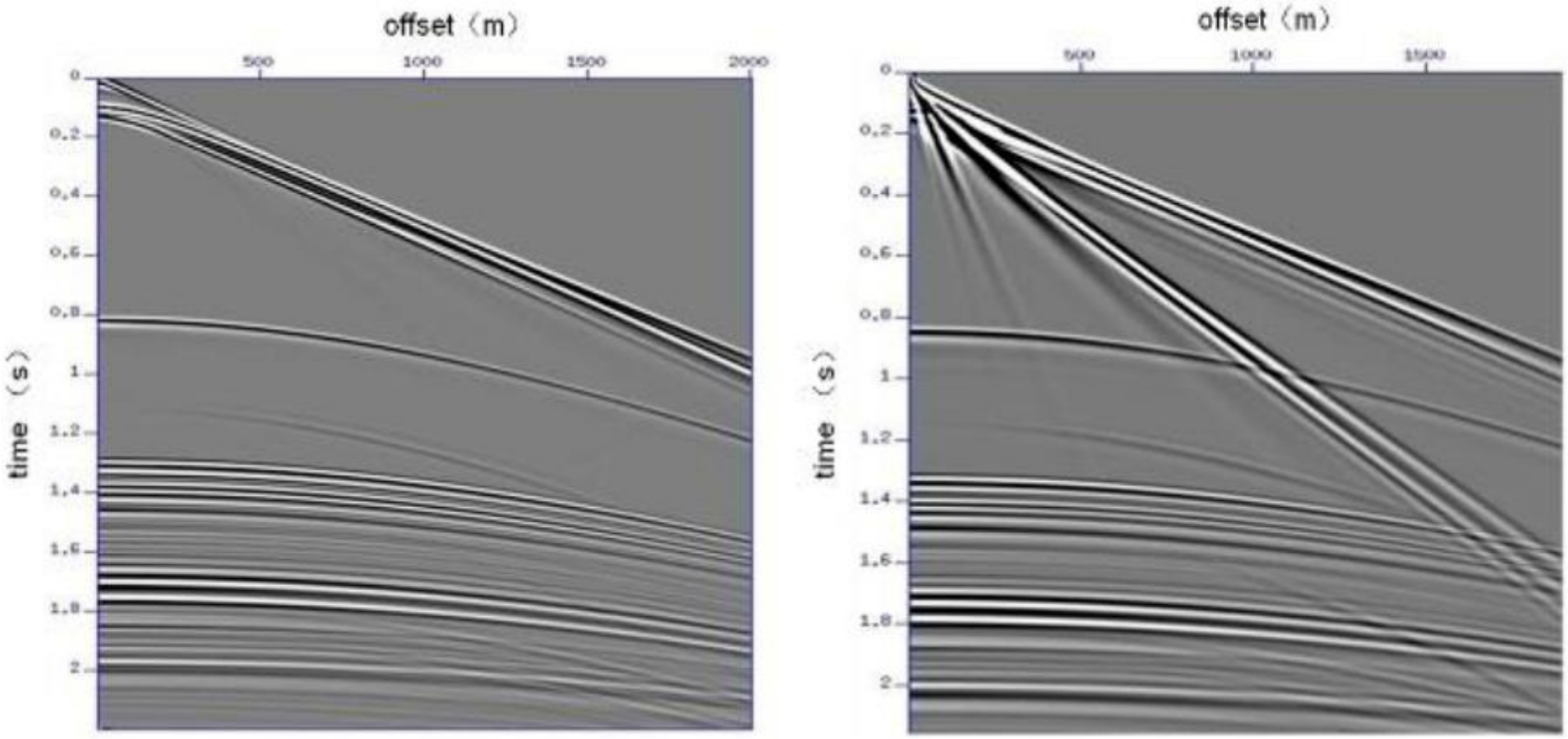

Figure 19. Energy extracted from the record (source dominant frequency 40Hz): without near surface (a: left) and with near surface (b: right).

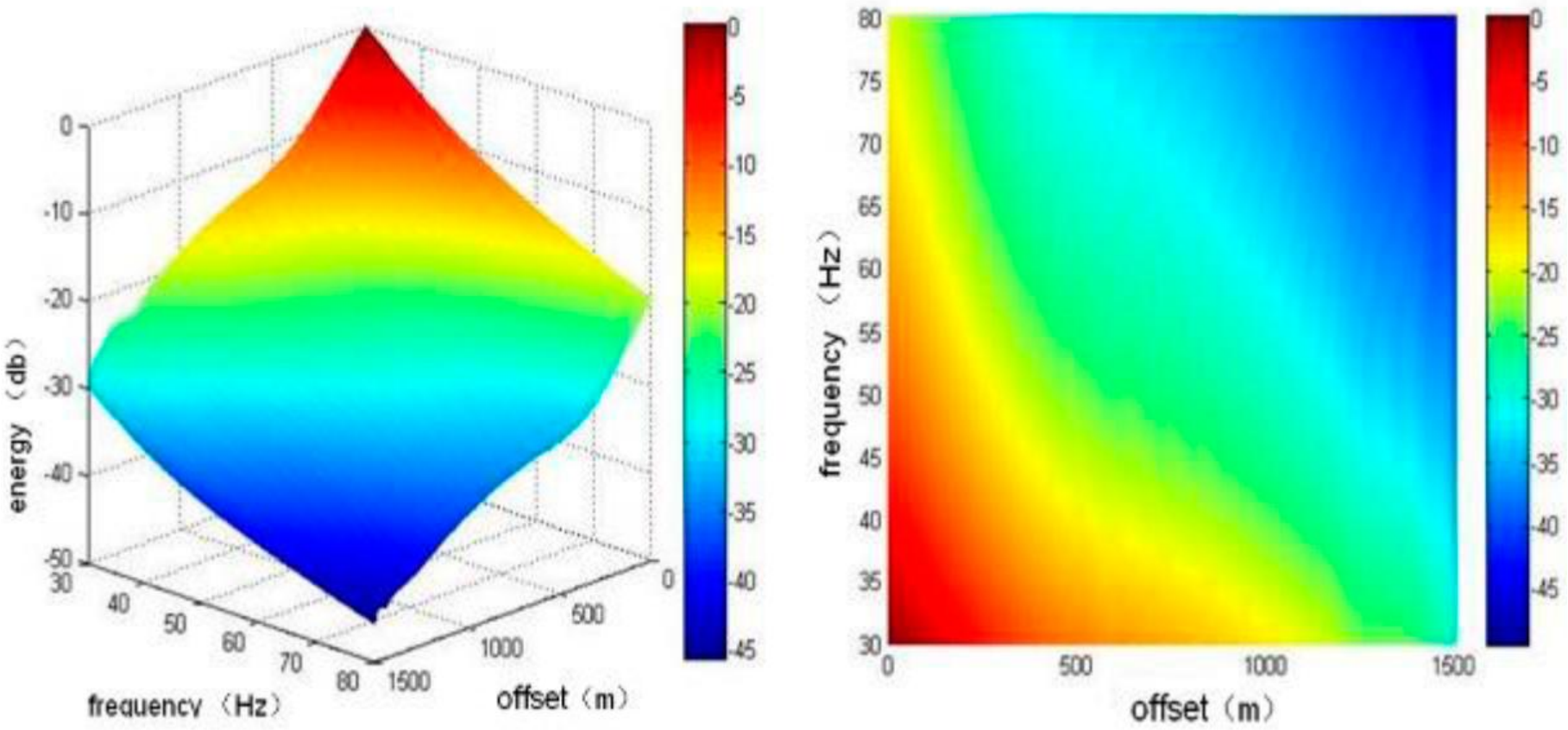

Figure 20. Relationship between energy, offset and source frequency (with near surface model): cubic view (a: left) and plane view (b: right).

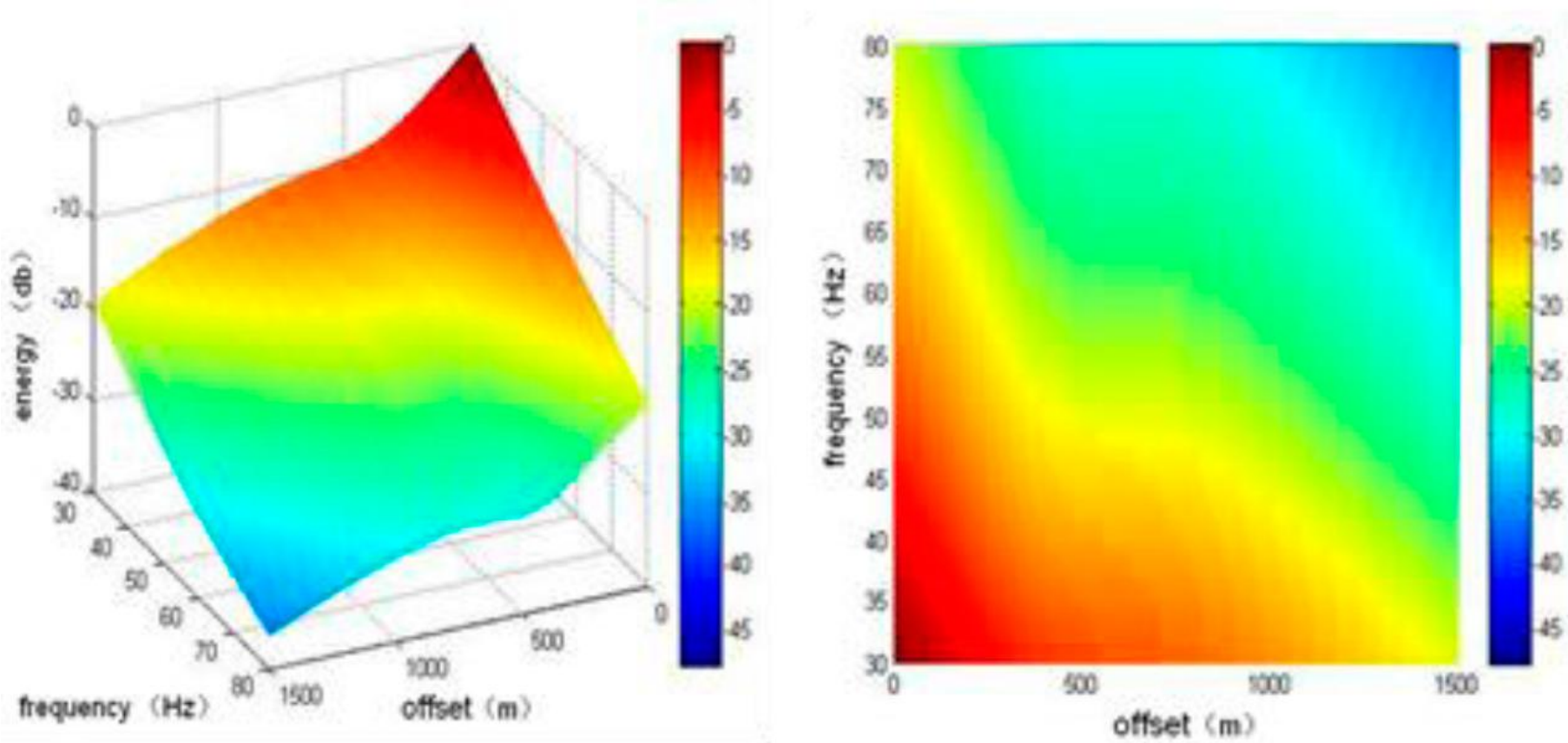

Figure 21. Relationship between energy, offset and source frequency (without near surface model): cubic view (a: left) and plane view (b: right).

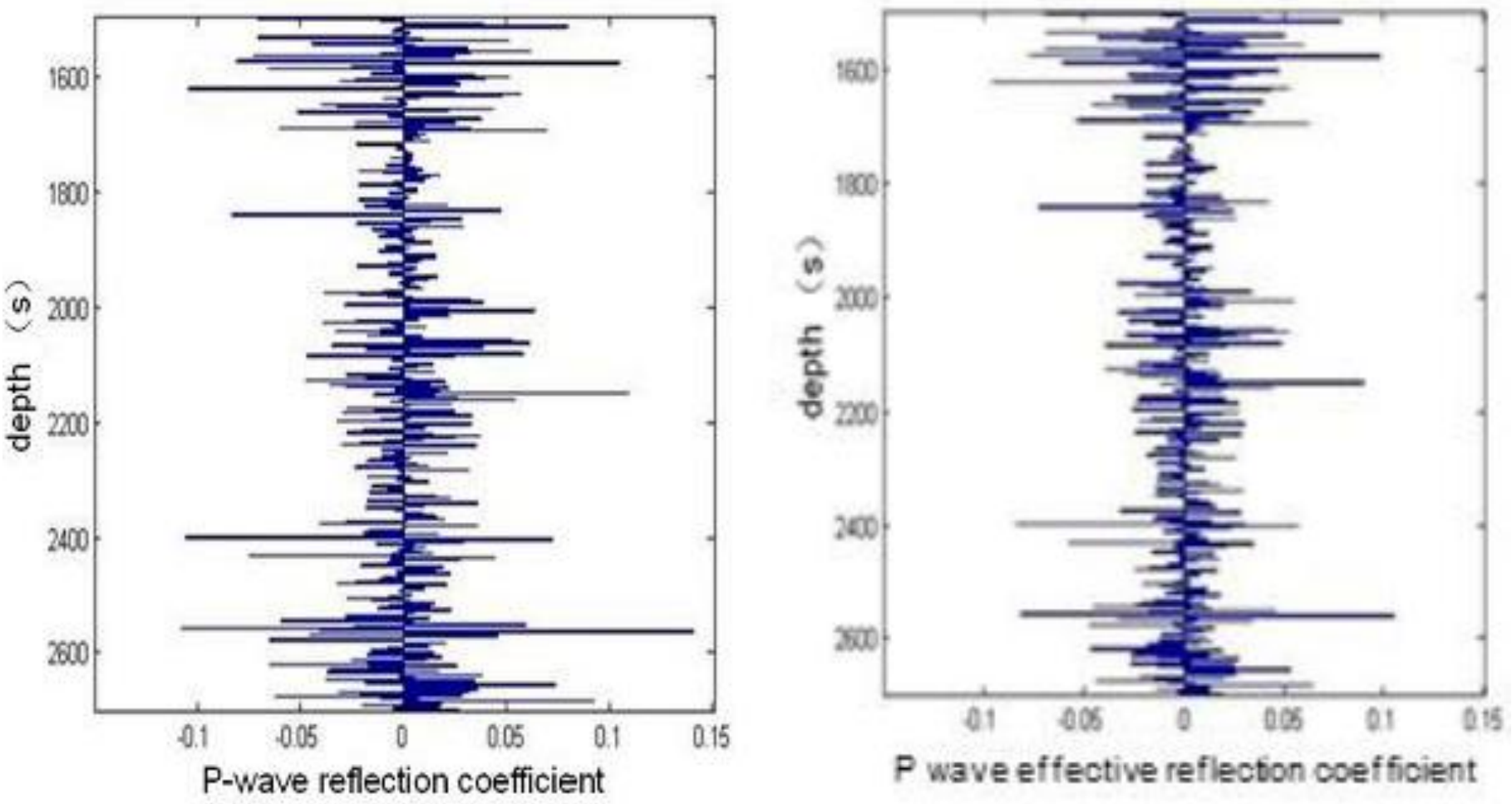

Figure 22. Reflection coefficient on deep layer: original reflection coefficient (a: left) and effective reflection coefficient (b: right).

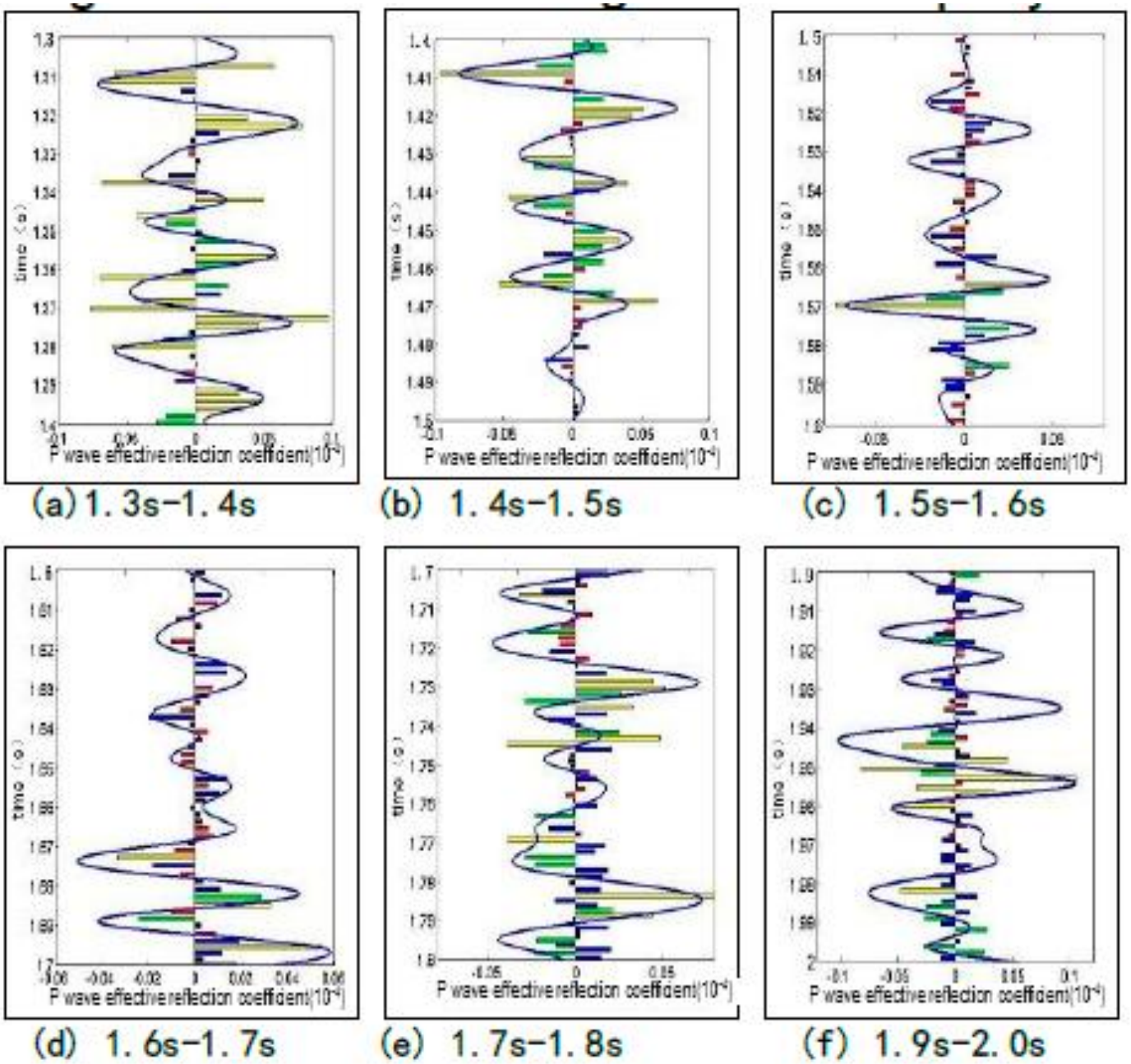

Figure 23. P wave effective reflection coefficient.

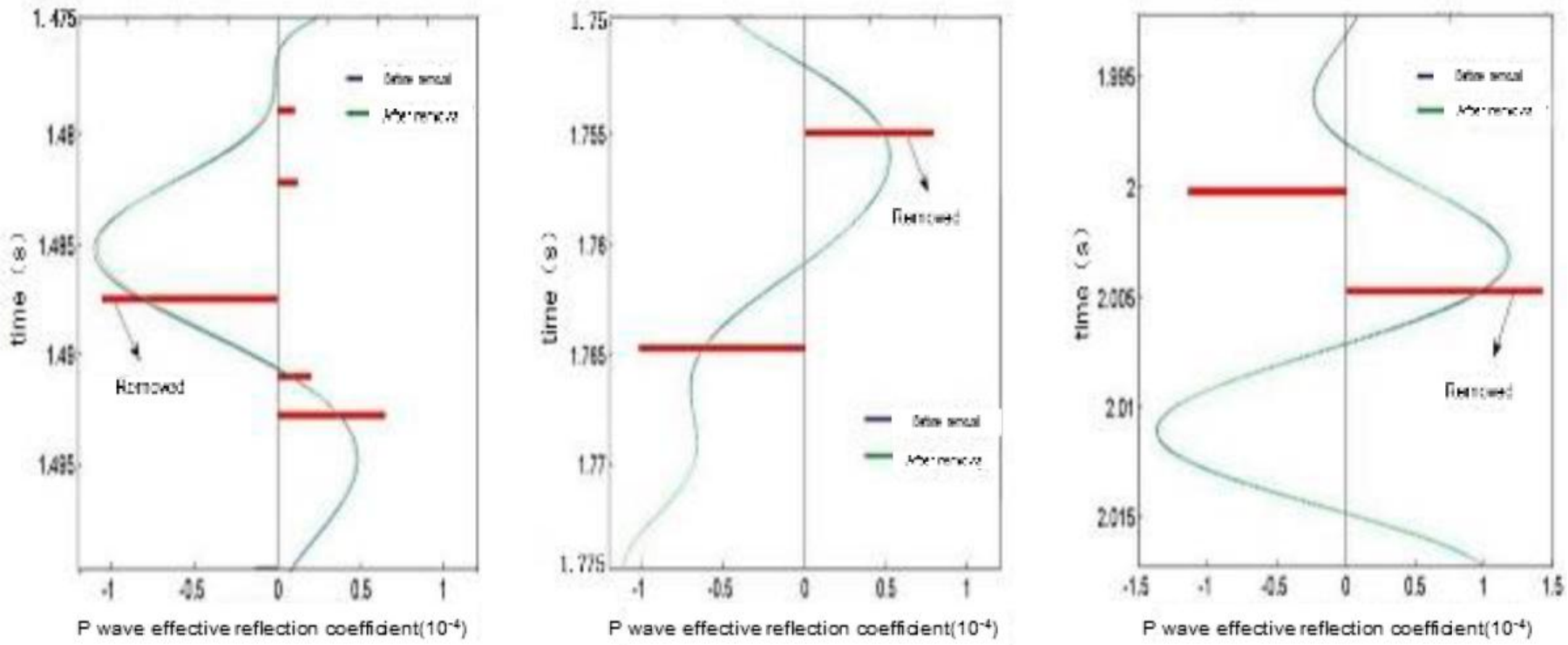

Figure 24. Record comparison after removing weak signal: 1,725m (a: left), 2,105m (b: middle), and 2,657m (c: right).